Air quality response in China linked to the 2019 novel Coronavirus (COVID-19) mitigation

K. Miyazaki[1], K. Bowman[1], T. Sekiya[2], Z. Jiang[3], X. Chen[3], H. Eskes[4], M. Ru[5], Y. Zhang[5], and D. Shindell[5,6]

[1]Jet Propulsion Laboratory, California Institute of Technology, Pasadena, CA, USA
[2]Japan Agency for Marine-Earth Science and Technology, Yokohama, 236-0001, Japan
[3]School of Earth and Space Sciences, University of Science and Technology of China, Hefei, Anhui, China
[4]Royal Netherlands Meteorological Institute (KNMI), De Bilt, the Netherlands
[5]Nicholas School of the Environment, Duke University, Durham, NC, USA
[6]Porter School of the Environment and Earth Sciences, Tel Aviv University, Israel

Key Points:

- We quantified the ancillary impacts of the COVID-19 mitigation on air pollution and human health using multiple satellite observations.
- Rapid reductions in Chinese NOx and SO_2 emissions increased surface ozone by 16 ppb over northern China but decreased PM2.5 nationwide.
- These changes increased about 2,100 ozone-related but decreased about 60,000 PM2.5-related incidences of morbidity.

Corresponding author: Kazuyuki Miyazaki, kazuyuki.miyazaki@jpl.nasa.gov

Abstract

Efforts to stem the spread of COVID-19 in China hinged on severe restrictions to human movement starting January 23rd, 2020 in Wuhan and subsequently to other provinces. Here, we quantify the ancillary impacts on air pollution and human health using inverse emissions estimates based on multiple satellite observations. We find that Chinese NOx emissions were reduced by 36% from early January to mid-February, with more than 80% of reductions occurring after their respective lockdown in most provinces. These emissions declines increased surface ozone by up to 16 ppb over northern China but decreased PM2.5 by up to 23 $\mu g\, m^{-3}$ nationwide. Air pollution appears to have substantially offset hospital admissions related to COVID-19, augmenting mitigation efforts, such as in the Hubei province with ∼400 reduced admissions. Changes in human exposure are associated with about 2,100 increased ozone-related morbidity incidences and avoidance of at least 60,000 PM2.5-related morbidity incidences.

Plain Language Summary

Satellite measurements such as TROPOMI have already captured the publics attention through remarkable images of pollutant reductions. However, the inference of emissions must account for variations in atmospheric transport, chemical environment, and meteorology. To that end, we developed an advanced chemical data assimilation system that incorporate these factors through ingestion of multiple chemical satellite and in-situ observations into chemical transport models, and quantified the reductions in emissions attributable to COVID-19 mitigation and determine the impact of those reduction on human health through pollutant exposure. We find that our Chinese NOx emission reductions had opposing air quality responses depending on timing and location. Our investigation shows opposing responses to morbidity in Northern China but compound impacts in Southern China, and that that air quality improvements actually augmented efforts to reduce hospital admissions.

1 Introduction

On January 23rd, 2020, 2 days before the Chinese New Year (CNY) celebration, the Chinese government imposed a "lock-down"in Hubei province which severely limited transportation and overall economic activity (Chinazzi et al., 2020; Li et al., 2020) until April 8th 2020 when the lockdown was lifted in Wuhan. These restrictions were designed to "flatten the curve" of disease transmission and consequently alleviate strain on the health care system (Wang et al., 2020). However, these mitigation efforts also had ancillary impacts on emissions of air pollutants, which represent the fifth highest mortality risk factor globally and are associated with about 4.9 million deaths in 2017 (Health Effects Institute, 2019). Particulate matter at 2.5 micron (PM2.5) and ozone are the primary contributors to air pollution. Ozone is formed through secondary photochemical production from precursor constituents such as hydrocarbons and carbon monoxide in the presence of nitrogen oxides (NOx), whereas PM is a widespread air pollutant including solid and liquid particles. During the 21st century China has become the epicenter of a dramatic redistribution of air pollutant emissions (Miyazaki et al., 2017; Zheng et al., 2018). Consequently, changes there could lead to substantial impacts on regional and potentially global air quality.

Satellite measurements, such as NO_2 columns from the Ozone Mapping Instrument (OMI) and the TROPOspheric Monitoring Instrument (TROPOMI), can readily capture synoptic changes in pollutants. However, the inference of emissions from these measurements must account for variations in atmospheric transport, chemical environment, and meteorology. To that end, advanced chemical data assimilation systems incorporate these factors through ingestion of multiple chemical satellite and in-situ observations into chemical transport models (CTMs) (Qu et al., 2019; Miyazaki et al., 2019, 2020b). The-

state-of-the-art data assimilation of multi-constituent observations has the potential to improve emission inversions by accounting for confounding factors in the relationship between emissions and concentrations, while reducing modelobservation mismatches arising from model errors unrelated to emissions (Miyazaki et al., 2017).

We estimate NOx and SO_2 emissions across all Chinese provinces accounting for the effects of emission reductions from CNY and the timing of lockdowns for each province. Changes in ozone and PM 2.5 are computed both within and between provinces. Consequently, health impacts, which we compute based upon population and exposure-response relationships (Liang et al., 2018), account for the effect of both local and non-local emissions changes. For these estimates, we use a multi-constituent satellite data assimilation (Miyazaki et al., 2020a), which simultaneously optimizes concentrations and emissions of various species while taking their complex chemical interactions into account.

2 Data and methods

An extended calculation of the Tropospheric Chemistry Reanalysis version 2 (TCR-2) (Miyazaki et al., 2020a) is used to evaluate emission and concentration changes (Text S1 and S2). The data products used in this study have been obtained from the assimilation of multiple satellite measurements of ozone, CO, NO_2, HNO_3, and SO_2 from the OMI, TROPOMI, MLS, and MOPITT satellite instruments (Text S3). The forecast model used is MIROC-CHASER (Text S4). An ensemble Kalman filter technique was used to optimizes both chemical concentrations of various species and emissions of several precursors. Surface measurements of NO_2, O_3, and PM2.5 concentration data from the national air quality monitoring stations (NAQMS) stations (Text S5) were used to evaluate the assimilation results. For short-term health impacts, we estimated respiratory hospital admissions and asthma-related emergency room visits for short-term ozone exposure, and children asthma symptom days, children bronchitis, respiratory hospital admissions, and cardiovascular hospital admissions for short-term PM2.5 exposure (Text S6).

3 Results

3.1 Anthropogenic emission reductions

Chinese emissions are typically low from January to February as a consequence of CNY. Climatological variations referenced to CNY in Fig. 1 are derived from our 16-year (2005-2020) emission time series (Miyazaki et al., 2020a). These reductions start about 20 days beforehand and reach their nadir after CNY before recovering about a month later. This recovery is reflected both in NOx emissions (13 % higher after the CNY holiday in the 2005-2019 average based upon a 14 day average) and NO_2 concentrations at the surface (+80.8 % in 2019, Table S1). Consequently, the mean CNY emissions are about 1.4 TgN/yr (daily emission values on a per year equivalent) less than the start of the year (9.0 TgN/yr) in the 2005-2019 average. Over the last decade, there have been significant trends in emissions. From 2005 to 2011 there was a 30% increase followed by rapid decrease after 2013 as a consequence of emissions controls (Cui et al, 2016; Miyazaki et al., 2017). However, these trends do not impact the relative reductions from the start of the year (less than 5 % multi-year spread).

In 2020, vehicle and industry activity were already affected by COVID-19 before the holidays (Kraemer et al., 2020) consistent with observed emission reductions. Right after the Wuhan lockdown and during the national holiday for CNY (January 24-February 2), emissions decreased by 0.9 TgN/yr to 6.2 TgN/yr, which is about 26 % lower than the value at the beginning of the year. The NOx emissions continued to decrease after the holidays and reached their minimum value of 5.5 TgN/yr on February 17, which is 36 % smaller than the early January value. The peak emission reduction in 2020 (2.9

TgN/yr) is about two times larger than that in the 2005-2019 average (1.4 TgN/yr). The reduction in 2020 corresponds to about 9 % of the global total anthropogenic emissions (33.4 TgN/yr) on a daily basis, which is comparable to the total emissions from Europe (4.1 TgN/yr), the United States (4.2 TgN/yr), or India (3.4 TgN/yr). Accounting for climatological variability, we attribute the additional 1.5 TgN/yr reduction to COVID-19 mitigation. By applying the average recovery rate per grid cell after January 23 (when the first lockdown was implemented), the accumulated emission amounts (total nitrogen emissions in NO_2 released to the atmosphere) during February 2020 is reduced by about 16 % using either the OMI assimilation (553 to 461 GgN) or the TROPOMI assimilation (378 to 316 GgN) using the same recovery rate linked to the COVID-19 mitigation. The relative emission changes derived using two instruments are consistent at country-scale (Table S2).

The baseline emission recovery for different provinces are shown in Fig 2a. We use the TROPOMI NO_2 assimilation results for the spatial analysis because of its better spatial coverage than OMI, while using the average recovery rate from the OMI records (Fig. 1). The recovery was on average about 3×10^{-6}kgN/m^2 with some provinces such as Zhejiang exceeding 20×10^{-6}kgN/m^2 after CNY. The impact of COVID-19 mitigation paints a very different picture. Rather than a recovery, provinces such as Zhejiang, Jiangsu, and Shandong along the eastern seaboard of China saw accumulated reductions exceeding 25×10^{-6} kgN/m^2 from January 23 to February 29 due to the COVID-19 mitigation (Fig. 2b). Spatially integrated country-wide totals show a reversal from +9 GgN (area-integrated emission sum of Fig. 2a and 2b) to -57 GgN due to mitigation based upon the TROPOMI assimilation. Similarly, OMI assimilation shows a reduction from -4 GgN to -100 GgN.

The NOx emission reductions are linked to the timing of the provincial lockdown. In the majority of provinces, 80% of reductions occurred after their respective lockdown (Fig 2d). For almost all provinces, 60% of reductions occurred after the lockdown. The relatively good linear relationship in Fig 3. of 2% per day reduction after the Wuhan lockdown (r=-0.78) suggest that the longer provinces waited to impose their own lockdown the more impact neighboring provinces had on local emissions reductions. In addition, the highest level of emergency announcement was issued on January 29 to all Chinese provinces, which likely affected economic activity before the actual implementation of provincial lockdowns, which sustained the lower emission levels at least until February 21 when the emergency level was lifted.

The reduction in NO_2 concentrations have significantly different spatial patterns than emissions (Table S3). The regional mean tropospheric NO_2 columns from TROPOMI retrievals show a north-south gradient with reductions of 50.6 % and 38.2 % for northeast and southeast China, respectively, from January 4-14 to February 14-24 whereas the estimated emission reductions are more uniform at 35.0 % and 37.1 %. The differences between emission and concentration reductions underscore the importance of non-linear chemistry (Miyazaki et al., 2020b). The north-to-south gradient in tropospheric NO_2 reductions is largely different between OMI (33.9 % and 42.0 %) and TROPOMI (50.6 % and 38.2 %), highlighting the influences of sampling and retrieval errors, whereas the estimated emission changes are consistent for the two instruments and not largely affected by the retrieval differences.

Similar to NOx emissions, the estimated SO_2 emissions exhibited a reduction and recovery pattern (Fig S1). The decreasing rate before the holiday is substantially larger in 2020 (-0.70 TgS/yr) than the climatological average (-0.12 TgS/yr). However, in contrast to a recovery in previous years (+0.32 TgS/yr), SO_2 emissions continue to decrease after the holiday (-0.24 TgS/yr for two weeks after the holiday). The maximum SO_2 emission reduction in January-February 2020 is 1.8 TgS/yr (by 29%, from 6.2 to 4.4 TgS/yr), which corresponds to about 5 % of the global total emissions (33.0 TgS/yr) and is comparable at an annual rate to the total emissions from India (1.8 TgS/yr). In contrast to NOx emissions, SO_2 emission reductions were concentrated in eastern and central China

(Fig. 2c), which could be attributed to different dominant emission categories. Power plant, industrial, and residential emissions dominate SO_2 emissions (Zheng et al., 2018). The northern and southern contrast could reflect the continued use of residential coal in the northern part, whereas reductions in emissions from the power and industry sectors could lead to the reductions in the southern part.

3.2 Air quality changes and short-term health impacts

In order to isolate the impact of COVID-19 mitigation on air pollutants, the 2020 emissions are adjusted based upon the difference between the 2015-2019 emission trends and 2020 emissions after CNY (Fig. S3). Our results show a bifurcated response in daily maximum 8-hour average (MDA8) ozone, which increased over central and northern China but decreased over southern China after the CNY holiday (Fig. 3a). The MDA8 responses reached 6 ppb for the February 15-25 average and 16 ppb for a single day over Hebei on February 19th and 20th. In particular, the Jiangsu province near Shanghai and Shandong province south of Beijing showed elevated responses exceeding 5 ppb for the February 15-25 average. Conversely, southern China broadly had reductions in ozone by around 1-5 ppb with higher reductions in coastal provinces in near Hong Kong in spite of broadly comparable NOx emission reductions. The opposing responses can be explained in part by the removal of ozone through NOx titration, which is enhanced by less efficient NOx transport from the boundary layer and a slower rate of photochemical ozone production predominant in winter seasons. This phenomenon is largely responsible for ozone increases during the cold season in response to decreased NOx emissions along with VOCs changes (Jhum et al., 2014).

These responses can differ significantly between chemical transport models. Those differences, however, can be diagnosed from our multi-model chemical data assimilation (Miyazaki et al., 2020b). The estimated ozone response (Text S7) had a factor of 2 difference among different models used within this framework due to fundamental differences in the representation of fast chemical and dynamical processes (Fig S4). For northern central China, the large negative responses range from 0.4-0.6 ppb per unit emission change ($10^{-11} kg N m^{-2} s^{-1}$). Even with a range of models, the multi-model differences in MDA8 simulations are smaller than 6 ppb for most regions (Miyazaki et al., 2020b), which is smaller than the evaluated model bias against the in-situ observations for most of eastern and southern China (Table S4). The biases suggest potential problems of many CTMs due to errors such as in dry deposition and VOCs emissions (Li et al., 2019). The uncertainty ranges in the Chinese NOx emissions due to model errors were quantified to be about 21% from the multi-model chemical data assimilation (Miyazaki et al., 2020b), while showing consistent temporal variations.

Nevertheless, these responses are broadly consistent with observed surface ozone changes as summarized in Table S4 and Fig S2 and described in Text S8, which can be explained by the combination of emissions (Fig S3) and background variability (i.e., synoptic and seasonal changes). The observed large increase in northeastern China is strongly related to the emission reductions. For some parts of southern China, both the observed and simulated ozone started to increase before the CNY holiday (Fig S2) and continued afterwards where the emission reductions do not solely explain the observed variability.

The PM2.5 response shows a strikingly different pattern than ozone (Fig 3d), with reductions of up to 10 $\mu g\, m^{-3}$ for the February 15-25 average and up to 23 $\mu g\, m^{-3}$ for a single day over Anhui on February 20th. Whereas the sign of the ozone response depends on region, the PM2.5 response to emissions decreases everywhere but are particular different in central China where provinces saw significant reductions such as Hubei (21 $\mu g\, m^{-3}$) and Henan (30 $\mu g\, m^{-3}$) (Table S4). In the model simulations, about 54, 92, and 71 % of the reductions in sulfate, nitrate, and ammonium aerosol concentrations were associated with SO_2 and NOx emission reductions after the 2020 CNY. However,

model responses underestimated PM2.5 relative to surface sites, especially over northeastern China (Table S4). These underestimates could be explained by the lack of observational constraints on direct aerosol emissions of organic and black carbon, and dust, and on other precursors such as NH_3 and VOCs. Because aerosol secondary formations can be initiated by OH-oxidation, changes in OH also affect the PM2.5 response. The surface OH concentrations were decreased by about 5-25 % in southern China and increased by 10-50 % in central and northern China, linked to the ozone and NOx changes (Fig S3). These are likely responsible for the relatively weak PM2.5 response in southern China, together with regional differences in removal processes. Aerosols have numerous impacts on surface ozone production and loss through heterogeneous chemical reactions, such as hydrolysis of N_2O_5, irreversible absorption of NO_2 and NO_3 on wet aerosols, and their influences on photolysis rate, which can reduce ozone by 8-20 ppb in northern and eastern China (Lou et al., 2014; Li et al., 2018; Li et al., 2019). Thus, the underestimated PM2.5 variations, along with other factors such as VOCs, could have impacts on temporal changes in ozone. However, the impact of aerosols heterogeneous reactions is complex, while the model considered N_2O_5 hydrolysis and HO_2 uptake but not NO_2 and NO_3 absorption on wet aerosols.

Reductions in ozone and PM2.5 from local emissions can impact pollutant distributions in other regions through atmospheric transport. We conducted a sensitivity calculation with changing emissions for five provinces in northern and eastern China (Zhejiang, Jiangsu, Shandong, Henan, and Hebei) where more than 70 % of contributions to total emission reductions occurred after lockdown. Corresponding to these emission changes, MDA8 and PM2.5 outside the five provinces were increased by up to 7 ppb and decrease by up to 6 $\mu g\, m^{-3}$, respectively, across East Asia including western Japan and Korean peninsula (Fig 3c and 3f). In southern China, the increases in ozone due to the non-local impacts compensated for parts of the ozone decreases due to the local emission reductions. For PM2.5, the non-local impacts lead to further reductions in southeastern China along with the local impacts.

The reductions in pollution from COVID-19 mitigation have a direct impact on human health, which are derived from population, baseline incidence rates for specific outcomes, and epidemiological exposure-response functions. Given the short window of the studied period, we focused our health impacts assessment on short-term effects associated with ozone and PM2.5. These short-term effects were characterized as morbidity, i.e. the disease, symptoms, and the required hospital and emergency room visits when necessary (Text S6). The short-term exposure changes linked to the COVID-19 mitigation were estimated using the ozone and PM2.5 simulation results with the standard and modified emissions. For ozone, total asthma-related emergency room visits for all age population and respiratory hospital admissions in post-65 population were estimated (Fig. 3b). For PM2.5, the number of respiratory and cardiovascular hospital admissions and cases of bronchitis in children ages 6-12 and asthma symptom days in children ages 5-19 were estimated (Fig. 3e). The total increase of 2,105 (905–3307, 95 % confidence levels) incidence of emergency room visits and hospital admissions due to ozone short-term exposure during 15-25 February is attributed to strong increases in northeastern China with the most impacts in Shandong, Henan, and Hebei (Table S5). The changes in PM2.5, associated with reductions in secondary formation processes in our estimates, led to a decrease of 60,691 (37,897–83,503) incidences of pm2.5-related asthma symptom days, cases of bronchitis, and hospital admissions with the top 3 contributions from Henan, Hunan, and Hebei (Table S5). In particular, changes in ozone and PM2.5 were associated with 5,017 reductions of respiratory and cardiovascular hospital admissions, with the top 3 contributions from Henan, Hunan, and Shandong (Table 1, Fig. 3b and 3e). These avoided hospital admissions were of the same order of magnitude as those needed for COVID-19 nationwide during the same period (∼2,165 based on an upper-limit estimate, Text S9). In Hubei, where the majority of COVID-19 hospitalization (∼2,019) occurred, the reduction of hospital admissions due to air quality was estimated as 406,

accounting for 20% of the upper-limit of COVID-19 hospital admissions. This implies that the air pollution declines in response to the lockdown likely had a substantial impact on the effectiveness of the lockdown in "flatten the curve" of disease transmission and consequently alleviate strain on the health care system. Although decisions of hospital admissions and emergency room visits can be complicated by changes in medical practices resulting from COVID-19 mitigation, the implications on health impacts we showed above are likely to be robust, given the distinct scale of estimates. Given the direct emissions of aerosols were not explicitly constrained in our estimate with consequent underestimates relative to observed changes (Table S4), the actual impacts of PM2.5 changes are likely even larger.

4 Conclusions and Discussion

The unprecedented steps taken to stop the transmission of COVID-19 had the ancillary effect of rapid reductions in NOx and SO2 emissions, from 8.4 TgN/yr in early January to only 5.5 TgN/yr in mid-February for NOx and from 6.2 TgS/yr to 4.4 TgS/yr for SO_2. These reductions provide insights but also challenges for future air quality policy and their interactions with chemistry-climate projections, which could be assessed with approaches like hierarchical emergent constraints (Bowman et al., 2018). Our results show that emission reductions can have opposing responses on different air pollutants and that policies in one location can affect emissions in another (Fig 3). Other emission sources not constrained in this study, such as VOCs and carbonaceous aerosols, are likely affected by COVID-19 mitigation but vary differently than NOx and SO_2 sources but are not as easily validated. Urban and rural chemistry along with point sources were not well separated here but could be improved in the future (Valin et al., 2011; de Foy et al., 2015).

Our results show that short-term health impacts were significant with increases of about 2,100 ozone-related but a decrease of about 60,000 PM2.5-related incidences of morbidity, with a decrease of about 5,000 hospital admissions. Henan was by far the greatest beneficiary of these reductions that was not directly reflected in the NO_2 concentration reduction (Table 1). On the other hand, Shandong was the most negatively impacted from ozone exposure even though it did not have the largest ozone response. These health outcomes need to be placed in the context of this extraordinary event. For example, actual exposure given limited movement may be different as the balance of indoor and outdoor exposure would not be typical. These reductions were entirely a consequence of emissions-related activity. Realizing similar improvements in emission efficiency would require significant changes in controls and technology. Nevertheless, the magnitude of estimated health impacts shows there are significant health benefits from such aggressive reductions in emissions that could serve as a basis for air quality planning in the future.

Acknowledgments

K.M. and K.B. acknowledge the support by the NASA Atmospheric Composition: Aura Science Team Program (19-AURAST19-0044). Part of this work was conducted at the Jet Propulsion Laboratory, California Institute of Technology, under contract with NASA. We acknowledge the use of data products from the NASA Aura and EOS Terra and Aqua satellite missions. We also acknowledge the free use of the tropospheric NO_2 column data from the SCIAMACHY, GOME-2, and OMI sensors from http://www.qa4ecv.eu and from TROPOMI. The TROPOMI NO_2 algorithm and data processors have been developed by KNMI under the NSO TROPOMI Science Contract, in cooperation with ESA. Sentinel-5 Precursor is an ESA mission on behalf of the European Commission (EC). The Earth Simulator was used for model simulations under the Strategic Project with Special Support of the Japan Agency for Marine-Earth Science and Technology.

References

Amsalu, E., T. Wang, H. Li, Y. Liu, A. Wang, X. Liu, L. Tao, Y. Luo, F. Zhang, X. Yang, X. Li, W. Wang, X. Guo, *Acute effects of fine particulate matter (PM2.5) on hospital admissions for cardiovascular disease in Beijing, China: a time-series study. Environ Health* **18**, 70 (2019)

Anenberg, S. C., D. K. Henze, V. Tinney, P. L. Kinney, W. Raich, N. Fann, C. S. Malley, H. Roman, L. Lamsal, B. Duncan, R. V. Martin, A. van Donkelaar, M.Brauer, R. Doherty, J.E. Jonson, Y. Davila, K. Sudo, J.C. Kuylenstierna, *Estimates of the Global Burden of Ambient, Ozone, and on Asthma Incidence and Emergency Room Visits. Environ Health Perspect.* **126**, 107004 (2018)

Boersma, K. F., H. J. Eskes, A. Richter, I. De Smedt, A. Lorente, S. Beirle, J. H. G. M. van Geffen, M. Zara, E. Peters, M. Van Roozendael, T. Wagner, J. D. Maasakkers, R. J. van der A, J. Nightingale, A. De Rudder, H. Irie, G. Pinardi, J.-C. Lambert, S. C. Compernolle, *Improving algorithms and uncertainty estimates for satellite NO_2 retrievals: results from the quality assurance for the essential climate variables (QA4ECV) project. Atmos. Meas. Tech.* **11**, 66516678, `https://doi.org/10.5194/amt-11-6651-2018` (2018)

Bowman, K. W., N. Cressie, X. Qu, A. Hall, *A hierarchical statistical framework for emergent constraints: Application to snowalbedo feedback. Geophysical Research Letters* **45**, 13,050-13,059. `https://doi.org/10.1029/2018GL080082` (2018)

Center for International Earth Science Information Network - CIESIN - Columbia University, *Gridded Population of the World, Version 4 (GPWv4): Population Count, Revision 11* (NASA Socioeconomic Data and Applications Center (SEDAC), `https://doi.org/10.7927/H4JW8BX5` (2018)

Chinazzi, M., J. T. Davis, M. Ajelli, C. Gioannini, M. Litvinova, S. Merler, A. Pastore y Piontti, K. Mu, L. Rossi, K. Sun, C. Viboud, X. Xiong, H. Yu, M. E. Halloran, I. M. Longini Jr., A. Vespignani, *The effect of travel restrictions on the spread of the 2019 novel coronavirus (COVID-19) outbreak. Science* **368**, 395-400 (2020)

Cui, Y., Lin, J., Song, C., Liu, M., Yan, Y., Xu, Y., and Huang, B., *Rapid growth in nitrogen dioxide pollution over Western China. 20052013, Atmos. Chem. Phys.* **16**, 62076221, doi:10.5194/acp-16-6207-2016 (2016)

de Foy, B., Z. Lu, D. G. Streets, L. N. Lamsal, B. N. Duncan, *Estimates of power plant NOx emissions and lifetimes from OMI NO_2 satellite retrievals. Atmospheric Environment*, **116**, 1-11 (2015)

Dee, D. P., S. M. Uppala, A. J. Simmons, P. Berrisford, P. Poli, S. Kobayashi, U. Andrae, M. A. Balmaseda, G. Balsamo, P. Bauer, P. Bechtold, A. C. M. Beljaars, L. van de Berg, J. Bidlot, N. Bormann, C. Delsol, R. Dragani, M. Fuentes, A. J. Geer, L. Haimberger, S. B. Healy, H. Hersbach, E. V. Hlm, L. Isaksen, P. Kllberg, M. Khler, M. Matricardi, A. P. McNally, B. M. Monge-Sanz, J.-J. Morcrette, B.-K. Park, C. Peubey, P. de Rosnay, C. Tavolato, J.-N. Thpaut, F. Vitart, *The ERA-Interim reanalysis: configuration and performance of the data assimilation system, Q. J. R. Meteorol. Soc.*, **137**, 553597, https://doi.org/10.1002/qj.828 (2011)

Deeter, M. N., D. P. Edwards, G. L. Francis, J. C. Gille, S. Martnez-Alonso, H. M. Worden, C. Sweeney, *A climate-scale satellite record for carbon monoxide: the MOPITT Version 7 product. Atmos. Meas. Tech.* **10**, 25332555, `https://doi.org/10.5194/amt102533-2017` (2017)

Efron, B., *Bootstrap Methods - Another Look at the Jackknife. Annals of Statistics* **7**, 126 (1979)

Global Burden of Disease Collaborative Network. *Global Burden of Disease Study 2017 (GBD 2017) Results.* (Seattle, United States: Institute for Health Metrics and Evaluation (IHME) (2018)

Graedel, T. E., T. S. Bates, A. F. Bouwman, D. Cunnold, J. Dignon, I. Fung, D. J. Jacob, B. K. Lamb, J. A. Logan, G. Marland, P. Middleton, J. M. Pacyna, M.

Placet, C. Veldt, *A compilation of inventories of emissions to the atmosphere. Global Biogeochem. Cy.* **7**, 126 (1993)

Health Effects Institute, *State of Global Air 2019*. www.stateofglobalair.org (2019)

Janssens-Maenhout1, G., M. Crippa1, D. Guizzardi, F. Dentener, M. Muntean, G. Pouliot, T. Keating, Q. Zhang, J. Kurokawa, R. Wankmller, H. Denier van der Gon, J. J. P. Kuenen, Z. Klimont, G. Frost, S. Darras, B. Koffi, and M. Li, *HTAP v2.2: a mosaic of regional and global emission grid maps for 2008 and 2010 to study hemispheric transport of air pollution. Atmos. Chem. Phys.* **15**, 1141111432, doi:10.5194/acp-15-11411-2015 (2015)

Jiang, Z., B. C. McDonald, H. Worden, J. R. Worden, K. Miyazaki, Z. Qu, D. K. Henze, D. B. A. Jones, A. F. Arellano, E. V. Fischer, L. Zhu, K. F. Boersma, *Unexpected slowdown of US pollutant emission reduction in the past decade. Proc. National. Acad. Sci.* **115**, 201801191 (2018)

Jhun, I., B. A. Coull, A. Zanobetti, P. Koutrakis, *The impact of nitrogen oxides concentration decreases on ozone trends in the USA. Air. Qual. Atmos. Health.* **8**, 283292. doi:10.1007/s11869-014-0279-2 (2014)

Katsouyanni, K., J. M. Samet, H. R. Anderson, R. Atkinson, A. Le Tertre, S. Medina, E. Samoli, G. Touloumi, R. T. Burnett, D. Krewski, T. Ramsay, F. Dominici, R. D. Peng, J. Schwartz, A. Zanobetti, HEI Health Review Committee, *Air pollution and health: a European and North American approach (APHENA). Res. Rep. Health. Eff. Inst.* **142**, 5-90 (2009)

Kraemer, M. U. G., C.-H. Yang, B. Gutierrez, C.-H. Wu, B. Klein, D. M. Pigott, Open COVID-19 Data Working Group, L. du Plessis, N. R. Faria, R. Li, W. P. Hanage, J. S. Brownstein, M. Layan, A. Vespignani, H. Tian, C. Dye, O. G. Pybus, S. V. Scarpino, *The effect of human mobility and control measures on the COVID-19 epidemic in China. Science* 10.1126/science.abb4218 (2020)

Krotkov, N. A., C. A. McLinden, C. Li, L. N. Lamsal, E. A. Celarier, S. V. Marchenko, W. H. Swartz, E. J. Bucsela, J. Joiner, B. N. Duncan, K. F. Boersma, J. P. Veefkind, P. F. Levelt, V. E. Fioletov, R. R. Dickerson, H. He, Z. Lu, D. G. Streets, *Aura OMI observations of regional SO2 and NO_2 pollution changes from 2005 to 2015. Atmos. Chem. Phys.* **16**, 46054629, `https://doi.org/10.5194/acp-1646052016` (2016)

Li, R., S. Pei, B. Chen, Y. Song, T. Zhang, W. Yang, J. Shaman, *Substantial undocumented infection facilitates the rapid dissemination of novel coronavirus (SARS-CoV2). Science* DOI: 10.1126/science.abb3221 (2020)

Li, J., X. Chen, Z. Wang, H. Y. Du, W. Yang, Y. Sun, B. Hu, J. Li, W. Wang, T. Wang, P. Fu, H. Huang, *Radiative and heterogeneous chemical effects of aerosols on ozone and inorganic aerosols over East Asia. Science of the Total Environment* **622**, 1327-1342 (2018)

Li, J., T. Nagashima, L. Kong, B. Ge, K. Yamaji, J. S. Fu, X. Wang, Q. Fan, S. Itahashi, H.-J. Lee, C.-H. Kim, C.-Y. Lin, M. Zhang, Z. Tao, M. Kajino, H. Liao, M. Li, J.-H. Woo, J. Kurokawa, Z. Wang, Q. Wu, H. Akimoto, G. R. Carmichael, Z. Wang, *Model evaluation and intercomparison of surface-level ozone and relevant species in East Asia in the context of MICS-Asia Phase III Part 1: Overview. Atmos. Chem. Phys.* **19**, 1299313015, `https://doi.org/10.5194/acp-19-12993-2019` (2019)

Li, K., D. J. Jacob, H. Liao, J. Zhu, V. Shah, L. Shen, K. H. Bates, Q. Zhang, S. Zhai, *A two-pollutant strategy for improving ozone and particulate air quality in China. Nature Geoscience* **12**(11), 906910 (2019)

Liang, C.-K., J. J. West, R. A. Silva, H. Bian, M. Chin, Y. Davila, F. J. Dentener, L. Emmons, J. Flemming, G. Folberth, D. Henze, U. Im, J. E. Jonson, T. J Keating., T. Kucsera, A. Lenzen, M. Lin, M. T. Lund, X. Pan, R. J. Park, R. B. Pierce, T. Sekiya, K. Sudo, T. Takemura, *HTAP2 multi-model estimates of premature human mortality due to intercontinental transport of air pollution and emission sectors. Atmos. Chem. Phys.* **18**, 1049710520,

https://doi.org/10.5194/acp-18-10497-2018 (2018)

Livesey, N., W. Read, P. Wagner, L. Froidevaux, A. Lambert, G. Manney, L. Milln Valle, H. Pumphrey, M. Santee, M. Schwartz, S. Wang, R. A. Fuller, R. F. Jarnot, B. W. Knosp, E. Martinez, R. R. Lay, *Version 4.2 x Level 2 data quality and description document.* Jet Propul, Tech. rep., Lab., Tech. Rep. JPL D-33509 Rev. D, Pasadena, CA, USA (Available from https://mls.jpl.nasa.gov/data/v4-2_data_quality_document.pdf) (2018)

Lou, S., H. Liao, B. Zhu, *Impacts of aerosols on surface-layer ozone concentrations in China through heterogeneous reactions and changes in photolysis rates. Atmospheric Environment* **85**, 123-138 (2014)

Miyazaki, K., H. Eskes, K. Sudo, K. F. Boersma, K. Bowman, Y. Kanaya, *Decadal changes in global surface NOx emissions from multi-constituent satellite data assimilation. Atmos. Chem. Phys.* **17**, 807837, https://doi.org/10.5194/acp-17-807-2017 (2017)

Miyazaki, K., K. W. Bowman, K. Yumimoto, T. Walker, K. Sudo, *Evaluation of a multi-model, multi-constituent assimilation framework for tropospheric chemical reanalysis. Atmos. Chem. Phys.* **20**, 931967, https://doi.org/10.5194/acp-20-931-2020 (2020b)

Miyazaki, K., Sekiya, T., Fu, D., Bowman, K. W., Kulawik, S. S., Sudo, K., Walker, T., Kanaya, Y., Takigawa, M., Ogochi, K., Eskes, H., Boersma, K. F., Thompson, A. M., Gaubert, B., Barre, J., Emmons, L. K., *Balance of emission and dynamical controls on ozone during KORUS-AQ from multi-constituent satellite data assimilation. J. Geophys. Res.-Atmos.* **124**, 387413, https://doi.org/10.1029/2018JD028912 (2019)

Miyazaki, K., K. Bowman, T. Sekiya, H. Eskes, F. Boersma, H. Worden, N. Livesey, V. H. Payne, K. Sudo, Y. Kanaya, M. Takigawa, K. Ogochi, *An updated tropospheric chemistry reanalysis and emission estimates, TCR-2, for 20052018. Earth Syst. Sci. Data Discuss.* https://doi.org/10.5194/essd-2020-30, in review (2020a)

Miyazaki, K., H. J. Eskes, K. Sudo, *Global NOx emission estimates derived from an assimilation of OMI tropospheric NO_2 columns. Atmos. Chem. Phys.* **12**, 22632288, https://doi.org/10.5194/acp-12-2263-2012 (2012)

NHFPC, *China health and family planning statistical yearbook* (Beijing, China, Peking Union Medical College Publishing House, 2016)

Orellano, P., N. Quaranta, J. Reynoso, B. Balbi, J. Vasquez, *Effect of outdoor air pollution on asthma exacerbations in children and adults: Systematic review and multilevel meta-analysis. PLoS One* **12**, e0174050 (2017)

Randerson, J. T., G. R. van der Werf, L. Giglio, G. J. Collatz, P. S. Kasibhatla, *Global Fire Emissions Database, Version 4, (GFEDv4).* ORNL DAAC, Oak Ridge, Tennessee, USA, https://doi.org/10.3334/ORNLDAAC/1293 (2018)

Spadaro, J. V., V. Kendrovski, G.S. Martinez, *Achieving health benefits from carbon reductions: Manual for CaRBonH calculation tool.* World Health Organization (2018)

Sekiya, T., K. Miyazaki, K. Ogochi, K. Sudo, M. Takigawa, *Global high-resolution simulations of tropospheric nitrogen dioxide using CHASER V4.0, Geoscientific Model Development*, **11**, 959988, https://doi.org/10.5194/gmd-11-959-2018 (2018)

Sudo, K., M. Takahashi, J. Kurokawa, H. Akimoto, CHASER: *A global chemical model of the troposphere 1. Model description, J. Geophys. Res.*, **107**, ACH 71ACH 720, https://doi.org/10.1029/2001JD001113 (2002)

Tian, Y., X. Xiang, J. Juan, J. Song, Y. Cao, C. Huang, M. Li, Y. Hu, *Short-term Effect of Ambient Ozone on Daily Emergency Room Visits in Beijing, China. Sci. Rep.* **8**, 2775 (2018)

Qu, Z., D. K. Henze, N. Theys, J. Wang, W. Wang, *Hybrid mass balance/4DVar joint inversion of NOx and SO2 emissions in East Asia. Journal of Geophysi-*

cal Research: Atmospheres **124**(14), 8203-8224 (2019)

Valin, L. C., A. R. Russell, R. C. Hudman, R. C. Cohen, *Effects of model resolution on the interpretation of satellite NO_2 observations. Atmos. Chem. Phys.*. **11**, 1164711655, https://doi.org/10.5194/acp-11-11647-2011 (2011)

van Geffen, J., K. F. Boersma, H. Eskes, M. Sneep, M. ter Linden, M. Zara, J. P. Veefkind, *S5P TROPOMI NO_2 slant column retrieval: method, stability, uncertainties and comparisons with OMI. Atmos. Meas. Tech.* **13**, 13151335, https://doi.org/10.5194/amt-13-1315-2020 (2020)

Verity, R., L. C Okell, I. Dorigatti, P. Winskill, C. Whittaker, N. Imai, G. Cuomo-Dannenburg, H. Thompson, P. G. T. Walker, H. Fu, A. Dighe, J. T Griffin, M. Baguelin, S. Bhatia, A. Boonyasiri, A. Cori, Z. Cucunub, R. FitzJohn, K. Gaythorpe, W. Green, A. Hamlet, W. Hinsley, D. Laydon, G. Nedjati-Gilani, S. Riley, S. van Elsland, E. Volz, H. Wang, Y. Wang, X. Xi, C. A Donnelly, A. C Ghani, N. M Ferguson, *Estimates of the severity of coronavirus disease 2019: a model-based analysis, The Lancet* Published online March 30, 2020, https://doi.org/10.1016/S1473-3099(20)30243-7 (2020)

Wang, Z., J. Wang, J. He, *PActive and Effective Measures for the Care of Patients With Cancer During the COVID-19 Spread in China. JAMA Oncol.* Published online April 01, 2020 doi:10.1001/jamaoncol.2020.1198 (2020)

Watanabe, S., T. Hajima, K. Sudo, T. Nagashima, T. Takemura, H. Okajima, T. Nozawa, H. Kawase, M. Abe, T. Yokohata, T. Ise, H. Sato, E. Kato, K. Takata, S. Emori, M. Kawamiya, *MIROC-ESM 2010: model description and basic results of CMIP5-20c3m experiments, Geosci. Model Dev.*, **4**, 845872, https://doi.org/10.5194/gmd-4-845-2011 (2011)

Wu, J., T. Zhong, Y. Zhu, D. Ge, X. Lin, Q. Li, *Effects of particulate matter (PM) on childhood asthma exacerbation and control in Xiamen, China. BMC Pediatr* **19**, 194 (2019)

Zhang, S., G. Li, L. Tian, Q. Guo, X. Pan, *Short-term exposure to air pollution and morbidity of COPD and asthma in East Asian area: A systematic review and meta-analysis. Environ. Res.* **148**, 15-23 (2016)

Zheng, B., D. Tong, M. Li, F. Liu, C. Hong, G. Geng, H. Li, X. Li, L. Peng, J. Qi, L. Yan, Y. Zhang, H. Zhao, Y. Zheng, K. He, Q. Zhang, *Trends in China's anthropogenic emissions since 2010 as the consequence of clean air actions. Atmos. Chem. Phys.* **18**, 1409514111, https://doi.org/10.5194/acp-18-14095-2018 (2018)

Zheng, X. Y., H. Ding, L. N. Jiang, S. W. Chen, J. P. Zheng, M. Qiu, Y. X. Zhou, Q. Chen, W. J. Guan, *Association between Air Pollutants and Asthma Emergency Room Visits and Hospital Admissions in Time Series Studies: A Systematic Review and Meta-Analysis. PLoS One* **10**, e0138146 (2015)

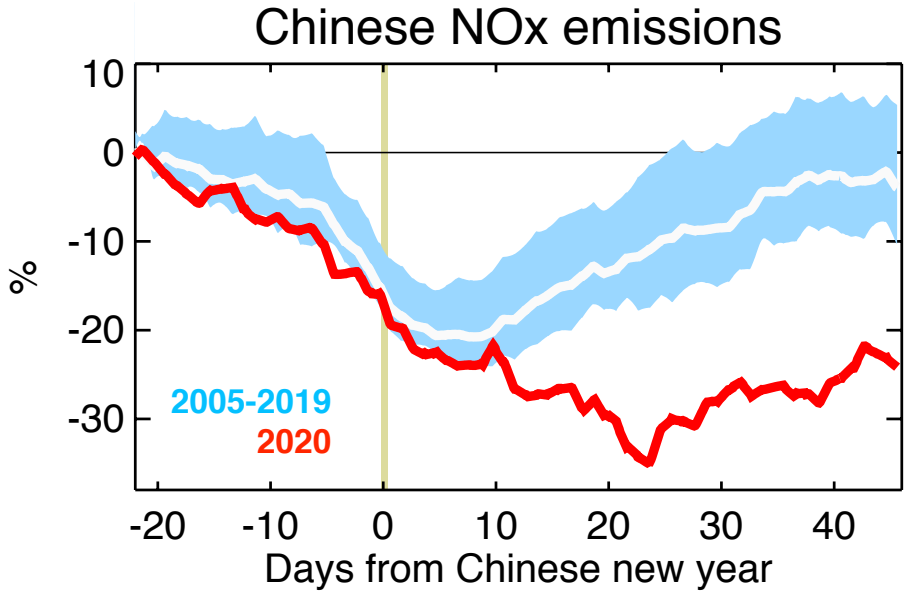

Fig. 1. Time series of relative changes in Chinese NOx emissions (in %) derived using OMI measurements as a function of days from CNY. The results are shown for 2005-2019 (average by while line and 1-σ standard deviation in light blue shade) and 2020 (red line).

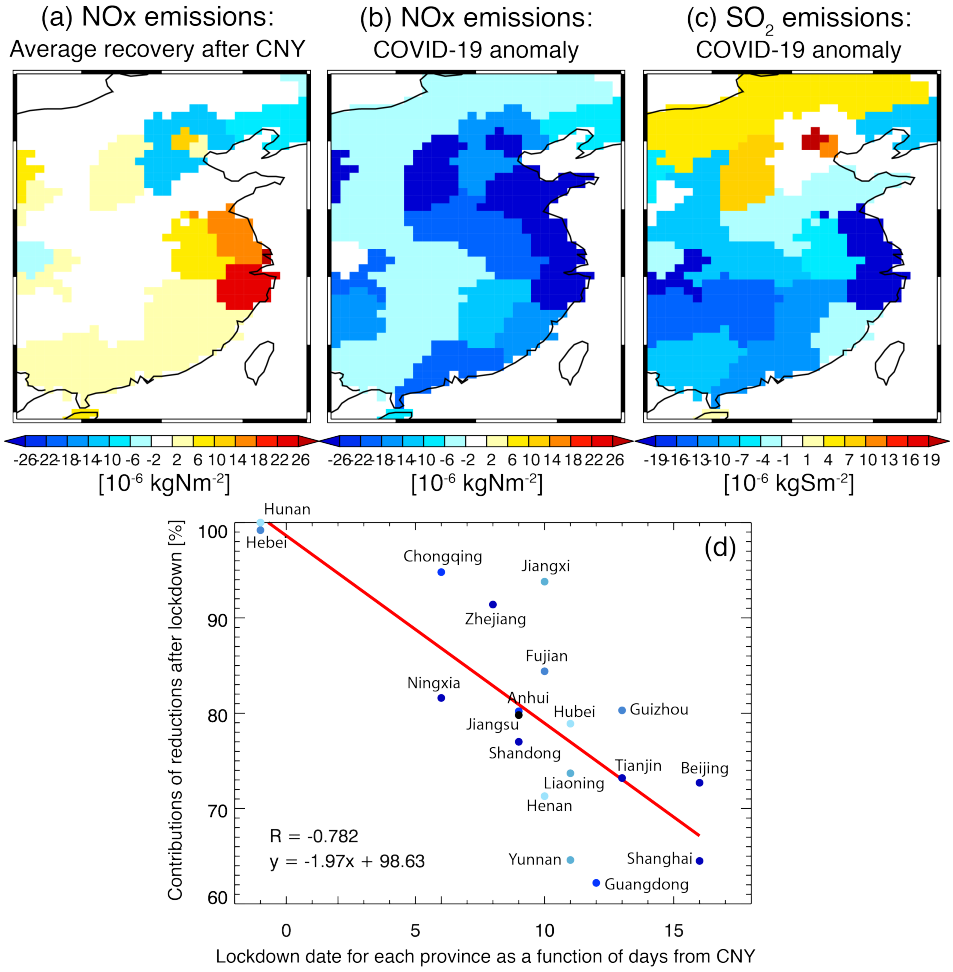

Fig. 2. Spatial distributions of the NOx and SO_2 total accumulated emission reductions from January 23 to February 29, 2020. The results are shown for (a) NOx emission changes due to average recovery rate for 2015-2019 and (b) due to COVID-19 anomaly, and (c) SO_2 emission changes due to COVID-19 anomaly. (d) shows contributions of emission reductions after lockdown to the total NOx emission reductions from January 23 to February 29, 2020 (in %) for each province as a function of days from CNY. The red line and numbers show linear regressions. Each dot represents each province, while the different colors represent accumulated emission reductions corresponding to the results in Fig. 2a and 2b.

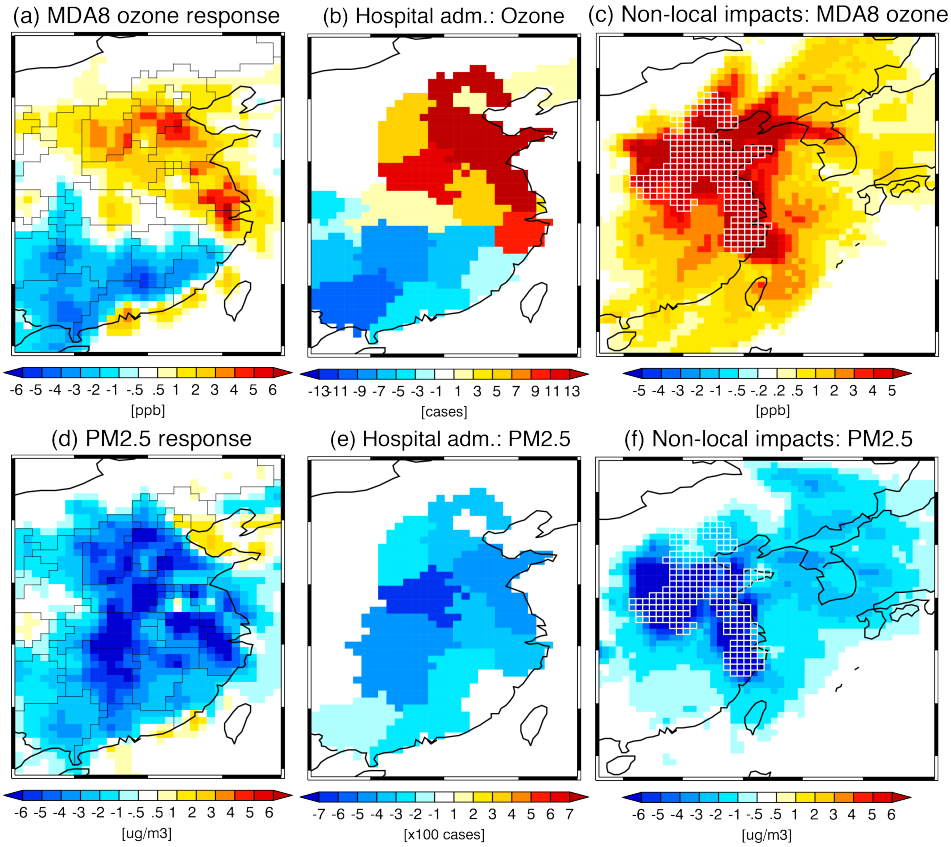

Fig. 3. Changes in (a) MDA8 (in ppb) and (d) PM2.5 concentrations (in $\mu g\, m^{-3}$) and (b,e) their impacts on short-term exposure linked to the COVID-19 mitigation during February 15-25, 2020. For (b) short-term ozone exposure, respiratory hospital admissions in post-65 population are shown. For (e) short-term PM2.5 exposure, the total number of respiratory and cardiovascular hospital admissions are shown. The results are also shown for maximum concentration changes at each grid point during February 15-25, 2020 in (c) MDA8 (in ppb) and (f) PM2.5 (in $\mu g\, m^{-3}$) linked to the COVID-19 mitigation for the five provinces in northeastern China (Zhejiang, Jiangsu, Shandong, Henan, and Hebei). The emission reductions were considered for the five provinces only in this case, which are marked by white mesh lines.

Table. 1. Total values of respiratory hospital admissions for short-term ozone exposure in post-65 population (Ozone HA), respiratory and cardiovascular hospital admissions for short-term PM2.5 exposure (PM2.5 HA), and new COVID-19 cases for February 15-25, 2020. Hospital admissions due to COVID-19 can be estimated based on the COVID-19 cases and the hospitalization fraction of COVID cases (∼2,165 cases for country total and ∼2,020 cases for Hubei based on an upper-limit estimate). The results are shown for selected provinces and country total.

Province	Ozone HA	PM2.5 HA	COVID-19 cases
Liaoning	1	-46	7
Beijing	3	-38	25
Tianjin	2	-1	15
Hebei	13	-371	21
Shanxi	6	-223	6
Shaanxi	1	-46	13
Shandong	17	-423	226
Jiangsu	-5	-243	27
Shanghai	3	-38	10
Anhui	6	-400	39
Henan	13	-696	63
Hubei	3	-406	10,976
Zhejiang	10	-338	43
Jiangxi	-5	-243	22
Hunan	-8	-500	15
Guizhou	-5	-79	3
Fujian	-3	-78	9
Guangdong	-4	-265	53
Guangxi	-11	-155	17
Total	60	-5,077	11,769

Figure 1.

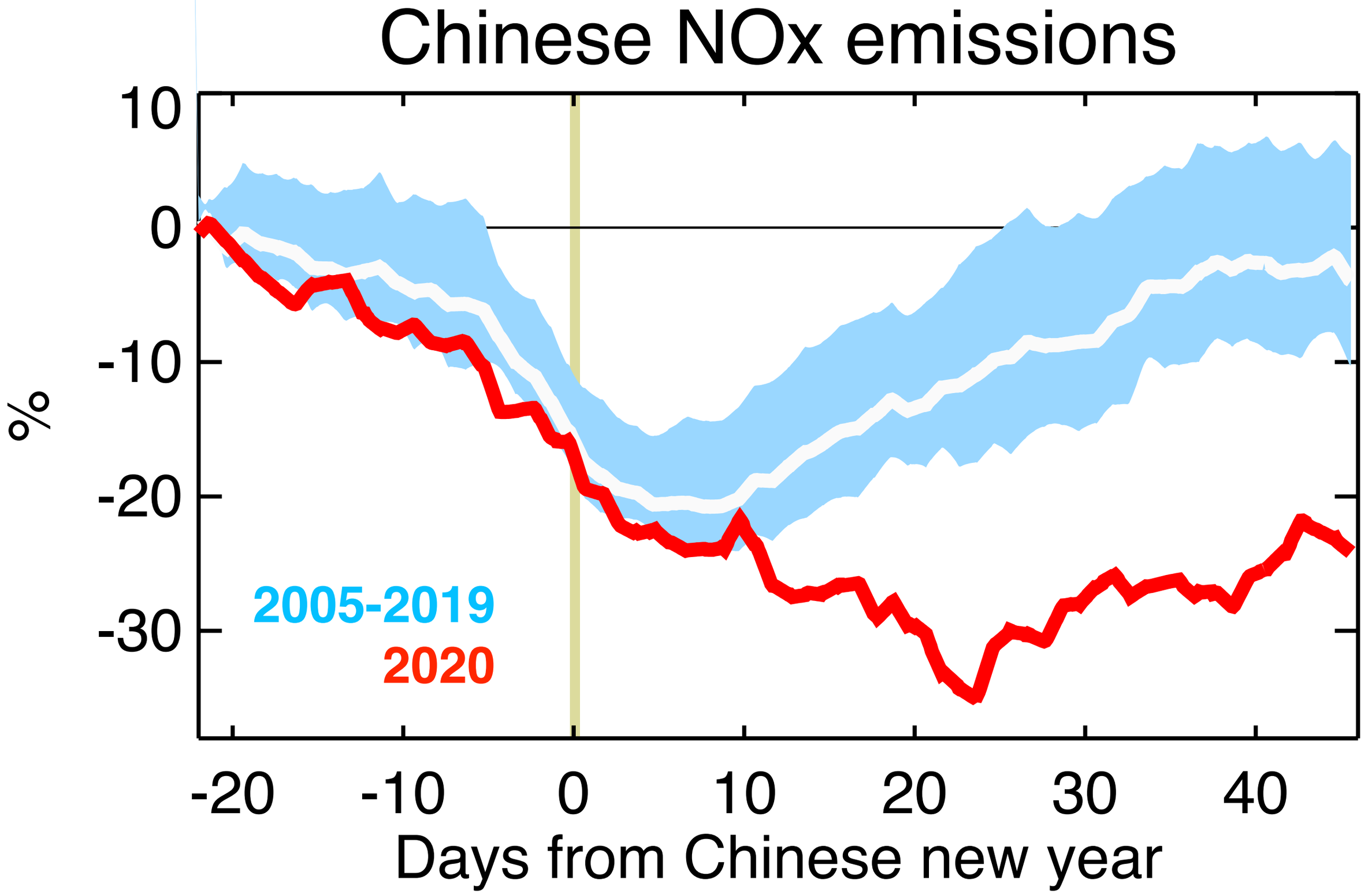
Chinese NOx emissions
10
0
-10
-20
-30
%
2005-2019
2020
-20
-10
0
10
20
30
40
Days from Chinese new year

Figure 2.

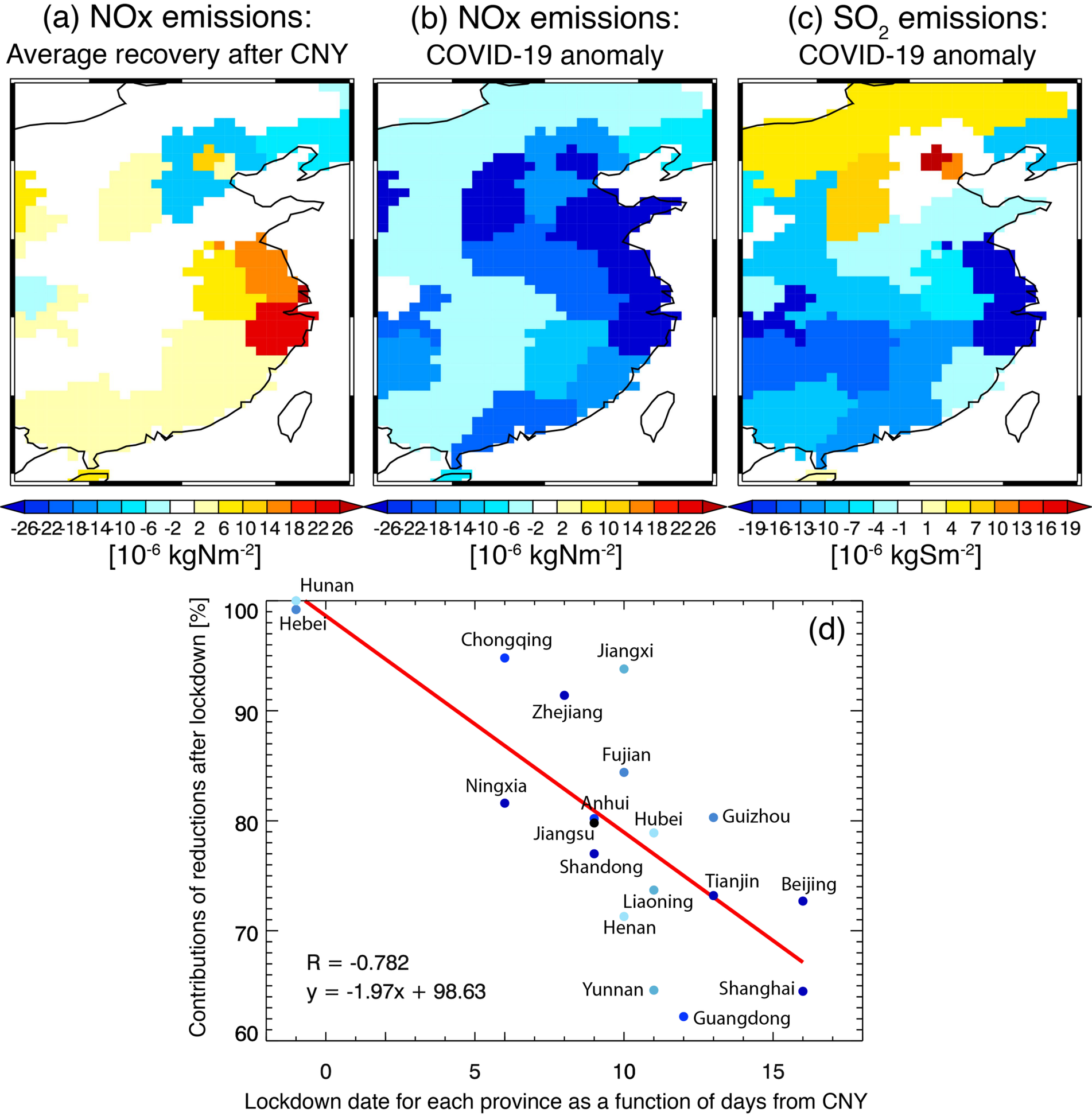
(a) NOx emissions:
Average recovery after CNY
(b) NOx emissions:
COVID-19 anomaly
(c) SO2 emissions:
COVID-19 anomaly
-26 -22 -18 -14 -10 -6 -2 2 6 10 14 18 22 26
[10-6 kgNm-2]
-26 -22 -18 -14 -10 -6 -2 2 6 10 14 18 22 26
[10-6 kgNm-2]
-19 -16 -13 -10 -7 -4 -1 1 4 7 10 13 16 19
[10-6 kgSm-2]
(d)
Contributions of reductions after lockdown [%]
Lockdown date for each province as a function of days from CNY
R = -0.782
y = -1.97x + 98.63
Hunan
Hebei
Chongqing
Jiangxi
Zhejiang
Fujian
Ningxia
Anhui
Hubei
Guizhou
Jiangsu
Shandong
Tianjin
Beijing
Liaoning
Henan
Yunnan
Shanghai
Guangdong
100
90
80
70
60
0
5
10
15

Figure 3.

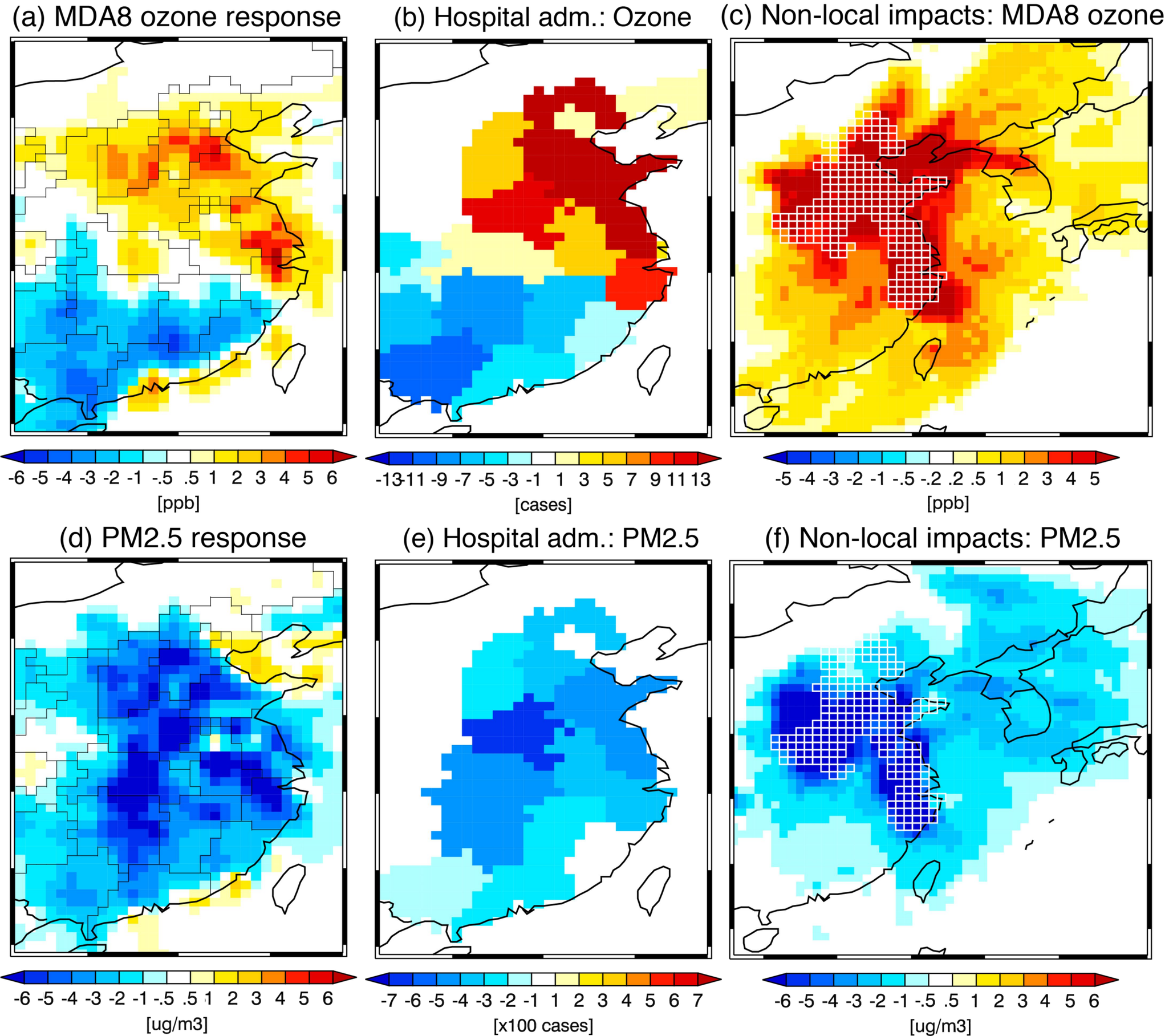
(a) MDA8 ozone response
-6 -5 -4 -3 -2 -1 -.5 .5 1 2 3 4 5 6
[ppb]
(b) Hospital adm.: Ozone
-13 -11 -9 -7 -5 -3 -1 1 3 5 7 9 11 13
[cases]
(c) Non-local impacts: MDA8 ozone
-5 -4 -3 -2 -1 -.5 -.2 .2 .5 1 2 3 4 5
[ppb]
(d) PM2.5 response
-6 -5 -4 -3 -2 -1 -.5 .5 1 2 3 4 5 6
[ug/m3]
(e) Hospital adm.: PM2.5
-7 -6 -5 -4 -3 -2 -1 1 2 3 4 5 6 7
[x100 cases]
(f) Non-local impacts: PM2.5
-6 -5 -4 -3 -2 -1 -.5 .5 1 2 3 4 5 6
[ug/m3]

Figure S1.

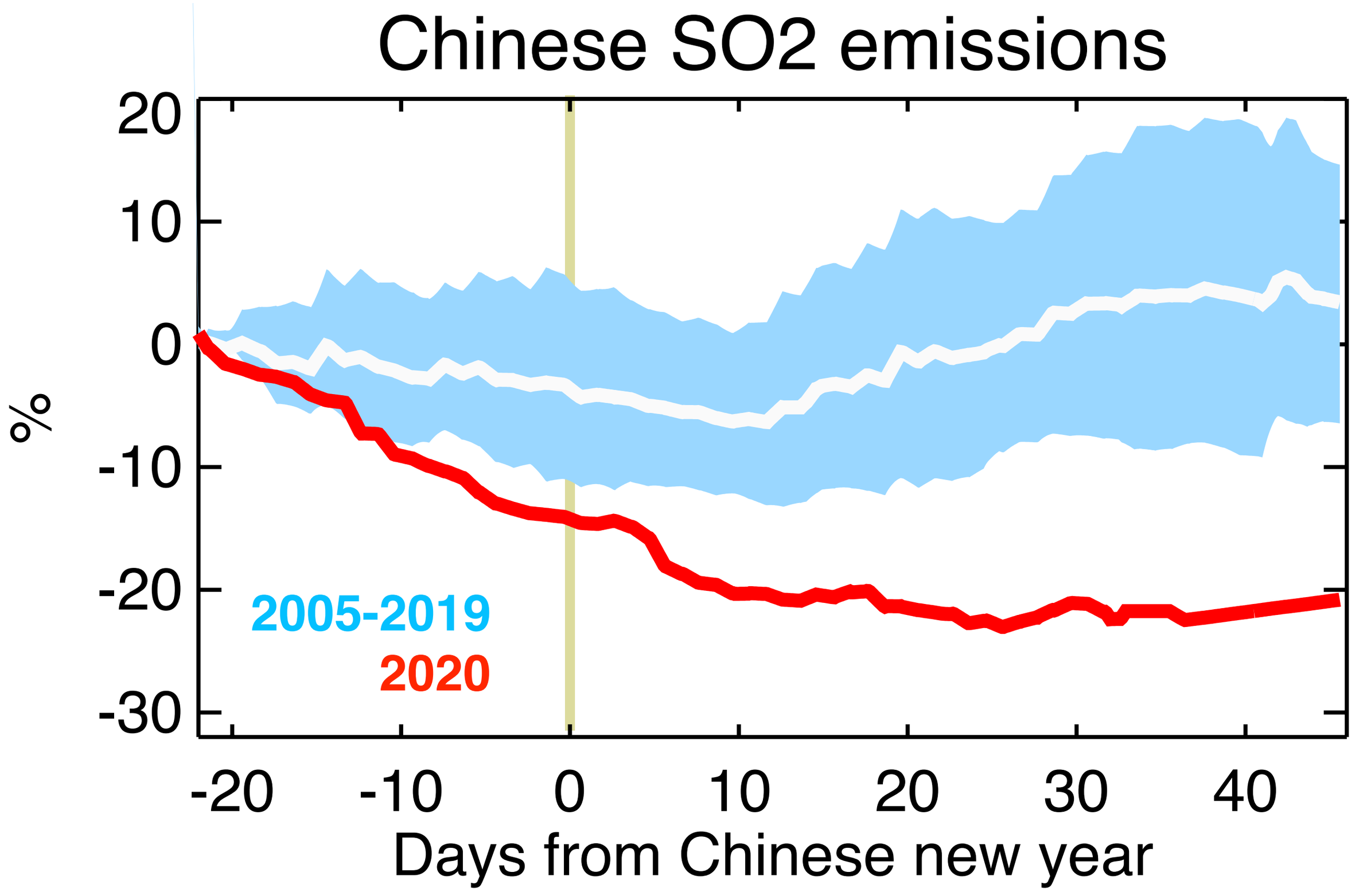
Chinese SO2 emissions
20
10
0
-10
-20
-30
%
2005-2019
2020
-20
-10
0
10
20
30
40
Days from Chinese new year

Figure S2.

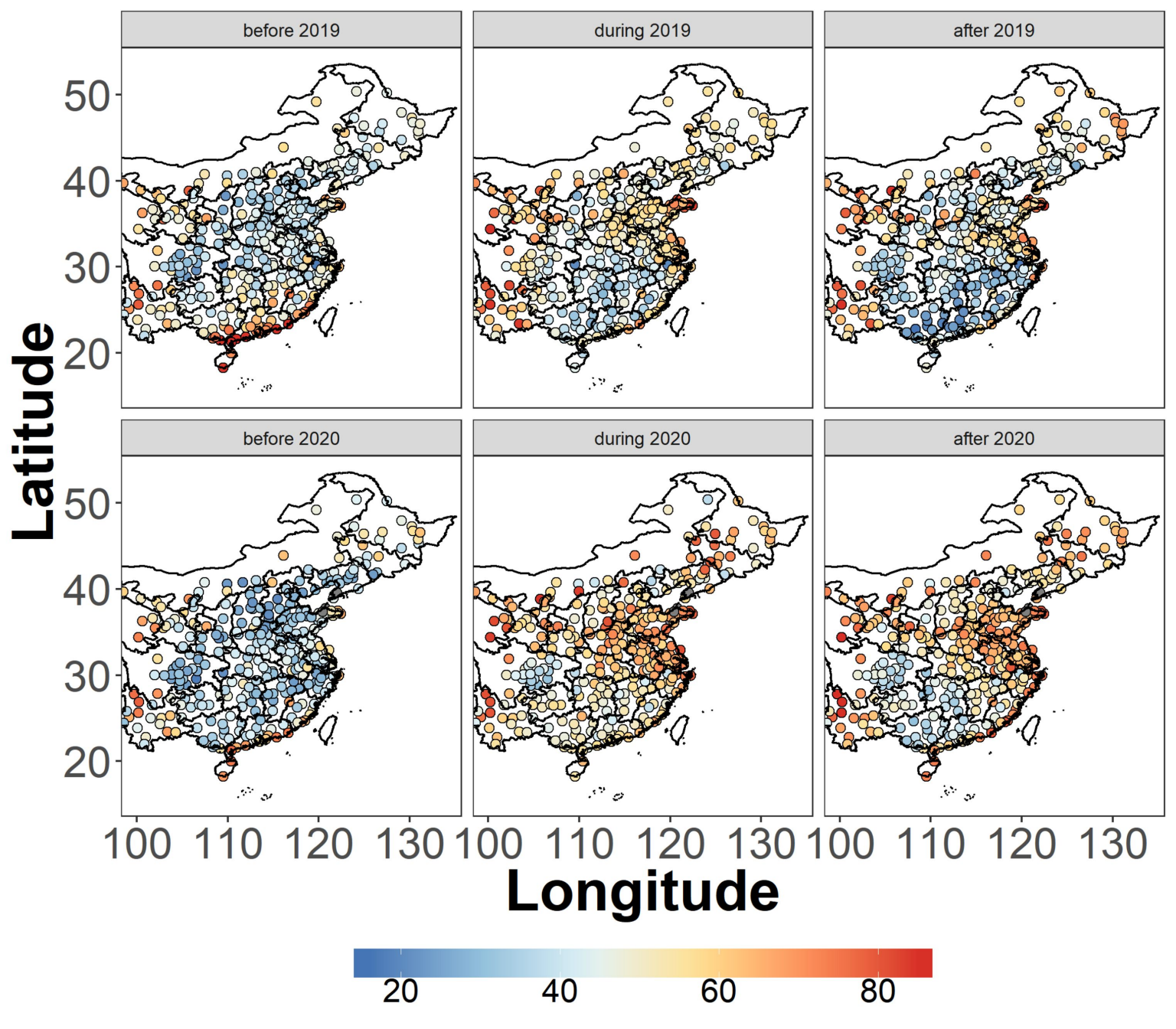
before 2019
during 2019
after 2019
before 2020
during 2020
after 2020
Latitude
50
40
30
20
100
110
120
130
Longitude
20
40
60
80

Figure S3.

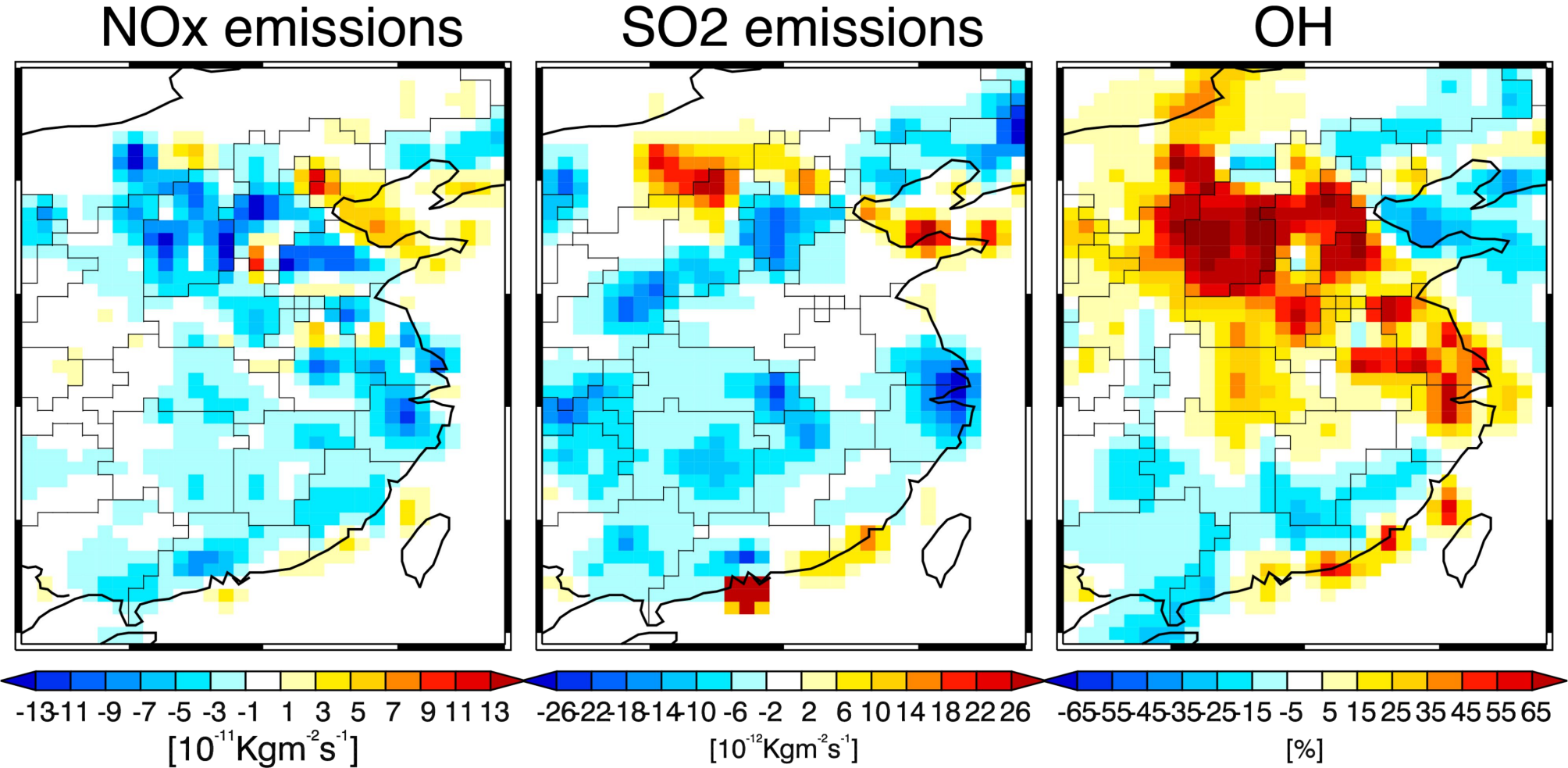
NOx emissions
SO2 emissions
OH
-13 -11 -9 -7 -5 -3 -1 1 3 5 7 9 11 13
[10^-11 Kgm^-2 s^-1]
-26 -22 -18 -14 -10 -6 -2 2 6 10 14 18 22 26
[10^-12 Kgm^-2 s^-1]
-65 -55 -45 -35 -25 -15 -5 5 15 25 35 45 55 65
[%]

Figure S4.

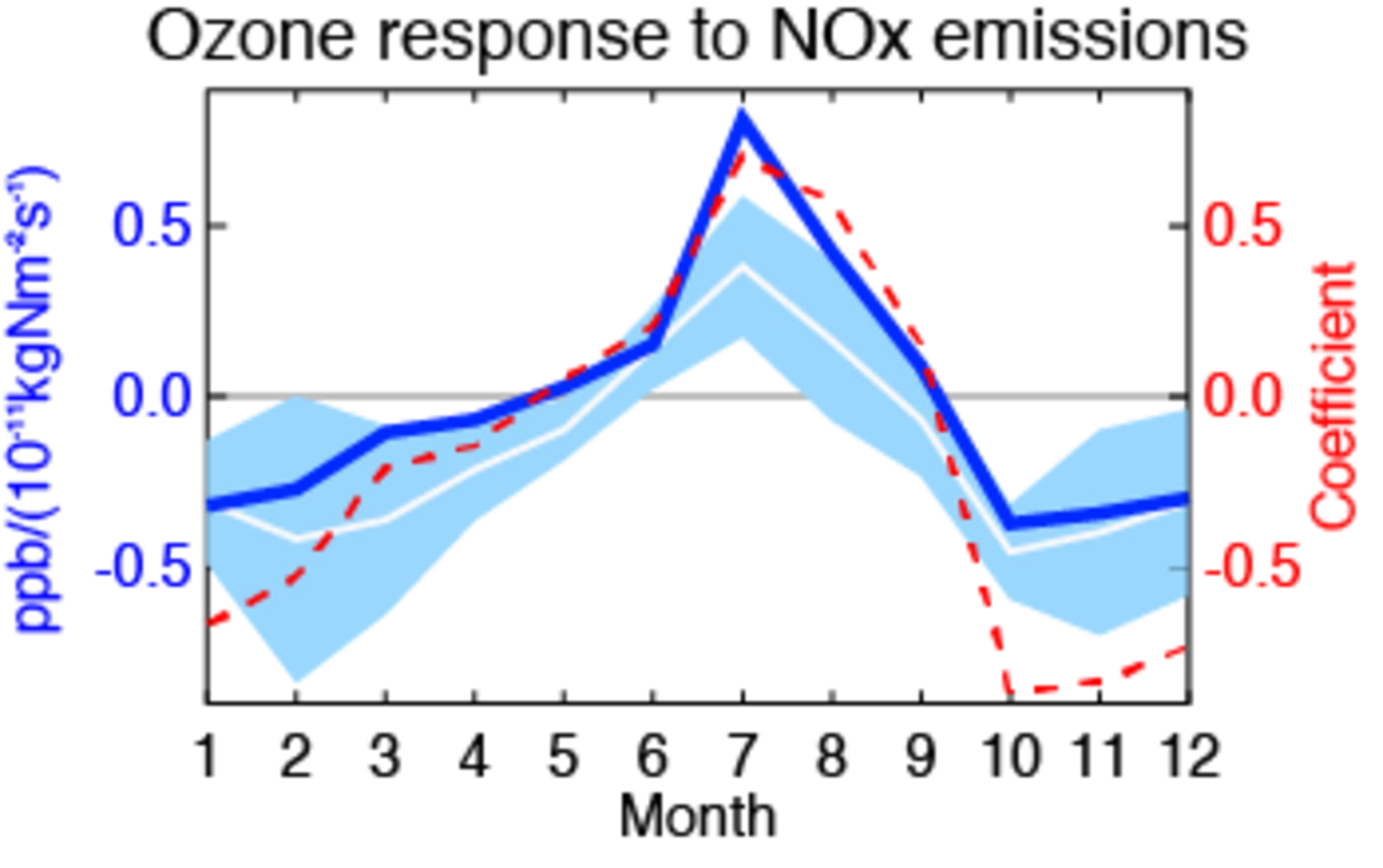
Ozone response to NOx emissions
ppb/(10⁻¹¹kgNm⁻²s⁻¹)
0.5
0.0
-0.5
Coefficient
0.5
0.0
-0.5
1 2 3 4 5 6 7 8 9 10 11 12
Month

Figure S5.

Before CNY

During CNY

After CNY

OMI

Assimilation

Model
(w/o assimilation)

Before CNY

During CNY

After CNY

TROPOMI

Assimilation

Model
(w/o assimilation)